International Scholarly Research Network
ISRN Renewable Energy
Volume 2011, Article ID 309496, 8 pages
doi:10.5402/2011/309496

Research Article

Risk-Constrained Unit Commitment of Power System Incorporating PV and Wind Farms

Sajjad Abedi, Gholam Hossein Riahy, Seyed Hossein Hosseinian, and Arash Alimardani

Renewable Energy Laboratory, Department of Electrical Engineering, Amirkabir University of Technology (Tehran Polytecnic), Hafez Avenue 424, Tehran 15875-4413, Iran

Correspondence should be addressed to Sajjad Abedi, sajjad.abedi@aut.ac.ir

Received 21 August 2011; Accepted 26 September 2011

Academic Editors: C. Lubritto, L. Ozgener, P. Poggi, and P. Tsilingiris

Wind and solar (photovoltaic) power generations have rapidly evolved over the recent decades. Efficient and reliable planning of power system with significant penetration of these resources brings challenges due to their fluctuating and uncertain characteristics. In this paper, incorporation of both PV and wind units in the unit commitment of power system is investigated and a risk-constrained solution to this problem is presented. Considering the contribution of PV and wind units, the aim is to determine the start-up/shut-down status as well as the amount of generating power for all thermal units at minimum operating cost during the scheduling horizon, subject to the system and unit operational constraints. Using the probabilistic method of confidence interval, the uncertainties associated with wind and PV generation are modeled by analyzing the error in the forecasted wind speed and solar irradiation data. Differential evolution algorithm is proposed to solve the two-stage mixed-integer nonlinear optimization problem. Numerical results indicate that with indeterminate information about the wind and PV generation, a reliable day-ahead scheduling of other units is achieved by considering the estimated dependable generation of PV and wind units.

1. Introduction

Nowadays, researches and applications of renewable energy sources, such as solar and wind is growing rapidly. Technological and economical progress of efficient and reliable wind turbines and photovoltaic (PV) panels as well as the concerns about environmental issues has contributed to large penetration of wind and solar energy in the power system. The exploitation level of wind energy in several countries in Europe has been reported to be up to 20% of the total annual demand [1]. With further developments in the PV technology and lower manufacturing costs, the outlook is that the PV power will possess a larger share of electric power generation in the near future. Grid-connected PV is ranked as the fastest-growing power generation technology [2]. Although the PV installation costs are still high, PV generates pollution-free and very cost-effective power which relies on a free and abundant source of energy [3]. However, the integration of these renewable sources into the power system exhibits challenges mainly due to their natural intermittency and limited predictability.

One of the most prominent issues regarding power system operation is optimal scheduling of the units or the unit commitment (UC) problem. The problem is referred to as a nonlinear, nonconvex, large-scale, mixed integer, and combinatorial problem [4], so that the efforts have always been made to introduce new alternative solution techniques and to enhance the solution quality and computational efficiency. The objective is to determine the on/off state and the amount of power generation for each unit in the system such that the overall system operation cost over the scheduling time period is minimized and the load demand and operational constraints for the system and units are met [5]. The presence of the solar and wind energy makes the problem more difficult and embeds the stochastic parameters into the problem to be handled. The amount of available wind and solar power should be inevitably estimated with a reliable level of accuracy. Moreover, additional power reserves are needed to maintain the operation of the system at the required stability margin. The scheduled system reserves support the generator outages and, in addition, the intermittent generations [6].

The literature on the UC problem is vast. Various solution methods including both classic and heuristic methods have so far been investigated and reported [7] as the optimization method for the solution of the thermal UC problem. Priority List (PL) [8], Lagrangian Relaxation (LR) [9], Particle Swarm Optimization (PSO) [4], Genetic Algorithm (GA) [10], and Shuffled Frog Leaping Algorithm (SFLA) [11] are the most recent work. Each of the reported methods has their own advantages and drawbacks. The methods have been evaluated by considering the UC as a determinate problem, although the same solution qualities may be affected when uncertainty considerations due to the load swings and renewable penetrations are involved in the problem.

Some studies have focused on the integration of wind power into the unit commitment problem. In [6], a stochastic cost model and a UC solution method in a wind-integrated power system considering the demand and wind generation uncertainties is presented. In [12], the focus is on the solution method whereas the uncertainty modeling of wind generation is not explored. In [13], the WILMAR model based on the scenario tree tool is suggested to study the effects of stochastic wind and load on the UC. The integration of considerable solar resources in power system is also of great concern in operation and planning decisions. Although the fluctuation rate of the wind power is more significant than that of solar power, it necessitates taking into consideration the solar estimation with a level of risk, especially when it comes to have a high range of solar power penetration. In this paper, solution of the UC with both wind and PV power consideration is under study.

In the remainder of this paper, we present a simple method based on the probabilistic confidence interval accompanied with the differential evolution algorithm to form a risk-constrained solution to the unit commitment incorporating the uncertainties of PV and wind turbine generation (WTG) in power system. The effectiveness of the method is illustrated by application results to a test system.

2. UC Problem Formulation

The aim of solving the UC problem is to determine when to start up and shut down thermal units so that the total operating cost is minimized during the scheduling horizon, while the system and the generator constraints are satisfied. The generation costs of PV and WTG from the public utility are the cheapest because they need no fuel. Accordingly, the fuel cost is the significant component of the total operation cost, normally modeled by a quadratic input/output curve, written as

$$\mathrm{FC}_i(P_i^t) = A_i + B_i \cdot P_i^t + C_i \cdot (P_i^t)^2. \tag{1}$$

The summation of fuel, start-up, and shut-down costs of the generating units form the total operation cost over the planning period, which is given by

$$\mathrm{TC} = \sum_{t=1}^{T}\sum_{i=1}^{N}(\mathrm{FC}_i(P_i^t) \cdot u(t)) + \mathrm{SU}_T + \mathrm{SD}_T, \tag{2}$$

where SU_T is the start-up cost modeled as a two-valued (hot start/cold start) staircase function and SD_T is the shut-down cost which is assumed zero [14]:

$$\mathrm{SU}_i = \begin{cases} \mathrm{CS}_i, & \text{if } \mathrm{DT}_i > M\mathrm{DT}_i + \mathrm{CSH}_i, \\ \mathrm{HS}_i, & \text{if } M\mathrm{DT}_i \le \mathrm{DT}_i \le M\mathrm{DT}_i + \mathrm{CSH}_i, \end{cases} \tag{3}$$

where DT_i is the down time of unit *i*.

The constraints in the optimization process are explained as follows.

(a) Thermal Unit Constraints

(i) the unit initial operation status (must run, fixed power, unavailable/available);

(ii) the rated range of generation capacity:

$$P_{i\min} < P_i^t < P_{i\max}; \tag{4}$$

(iii) ramp up/down rates:

$$P_{i\max}^t = \min\left\{P_{i\max}, P_i^{t-1} + \tau \cdot \mathrm{RU}_i\right\}, \tag{5}$$

$$P_{i\min}^t = \max\left\{P_{i\min}, P_i^{t-1} - \tau \cdot \mathrm{RD}_i\right\}; \tag{6}$$

(iv) the minimum up/down time limits of the units.

This constraint represents the minimum time for which a unit must remain on/off before it can be shut down or restarted, respectively:

$$\begin{aligned} T_{i\mathrm{on}}^c &> M\mathrm{UT}_i\ , \\ T_{i\mathrm{off}}^c &> M\mathrm{DT}_i\ , \end{aligned} \tag{7}$$

where c is the number of the cycle among all cycles (C) which the scheduling horizon consists of. The summation of $T_{i\mathrm{on}}^c$ and $T_{i\mathrm{off}}^c$ over the whole cycles for each unit must be equal to the scheduling horizon (T) which is 24 hours:

$$\sum_{c=1}^{C}\left(T_{i\mathrm{on}}^c + T_{i\mathrm{off}}^c\right) = T. \tag{8}$$

(b) Renewable Power Risk Constraint. As mentioned before, the scheduling of power system in the presence of PV and WTG units requires estimation of their available power over the scheduling period. Nevertheless, even the most precise prediction methods reveal errors compared to actual data. From the viewpoint of secure operation scheduling of power system, the important factor is to confine the generation risks and uncertainties to a definite level and ensure a level of confidence about the intermittent power. The maximum power at risk will be calculated based on the desired level of confidence (LC) defined by the operator. The risk constraint is written as follows:

$$P\left(\mathrm{Power}_{\mathrm{risk}} \le \mathrm{Power}_{\mathrm{risk,max}}\right) > LC, \tag{9}$$

where $P\,(\text{Power}_{\text{risk}} < \text{Power}_{\text{risk,max}})$ indicates the probability of the power at risk ($\text{Power}_{\text{risk}}$) being less than the maximum power at risk $\text{Power}_{\text{risk,max}}$. $\text{Power}_{\text{risk,max}}$ is calculatedbased on LC and the probability density function (PDF) of the historical forecast errors, described in Section 3.2.

(c) System Constraints

(i) the system hourly power balance:

$$\sum_{i=1}^{N} u_i(t) \cdot P_i^t + P_{\text{C,RES}}(t) = D^t; \tag{10}$$

(ii) the spinning reserve (10-min) requirements;

$$\sum_{i=1}^{N} u_i(t) \cdot P_{i\max}^t \geq D^t + R^t, \tag{11}$$

where $P_{i\ \max}^t$ is obtained using (5) with $\tau = 10$.

The overall fitness function is written as:

$$\text{FF} = \text{TC} + \text{PT}, \tag{12}$$

where PT is the total penalty term ($\text{PT} = \text{PT}_{\text{res}} + \text{PT}_{\text{cap}}$) for penalizing the spinning reserve constraint violations PT_{res} and also the excessive capacity PT_{cap}, expressed by:

$$\begin{aligned} \text{PT}_{\text{res}} &= \sum_{t=1}^{T} \Re\left((D^t + R^t) - \sum_{i=1}^{N} u_i(t) \cdot \ P_{i\max}^t \right), \\ \text{PT}_{\text{cap}} &= \sum_{t=1}^{T} \Re\left(\sum_{i=1}^{N} u_i(t) \cdot P_{i\min}^t \ - D^t \right). \end{aligned} \tag{13}$$

3. Renewable Power Risk Analysis

3.1. Wind and Solar Power Prediction. The day-ahead prediction is generally used for power plant scheduling and electricity trading [6]. The power from uncertain units can be generally predicted by a variety of tools. Among these tools, the artificial neural network (ANN) which is wellknown and widely used for time series predictions [15, 16] is utilized in this study. In this study, an MLP network has been chosen because of the ease of application particularly compared with other hybrid ANNs (e.g., ANFIS, GA-ANN, etc.) [16]. Moreover, all needed functions are already available in the MATLAB neural networks toolbox.

The MLP network is trained using levenberg-marquardt technique which is fast for practical problems compared with other back-propagation algorithms such as gradient decent. Two independent networks are trained for solar and wind power prediction. The appropriate number of hidden neurons of each network determined using a forward heuristic simulation [15]. The number of neurons is initialized by a small number and incrementally changed in an iterative process to reach a point at which no significant advance is observed by increasing the number of hidden neurons. At such a point, a compromise between memorization and generalization ability is reached. The developed NNs have one output containing a vector of renewable power for 24 hours day ahead. The historical data of wind speed and solar irradiation is considered as the input parameters of the forecast. Figures 1 and 2 show a sequence of 24-hour actual and forecasted data as well as the forecast errors distribution of wind and solar power for one week, respectively. It can be seen that for long-term operation, the forecast errors are likely normally distributed [17]. The error data is obtained as the difference between the actual and estimated data:

$$\text{Err} = X_{\text{actual}} - X_{\text{estimated}}. \tag{14}$$

3.2. Risk Analysis. Models that consider the generation from wind and solar units completely deterministic ignore the additional problems that forecast uncertainty embeds in the system, while those that do not include meteorological forecasts may overvalue the costs. Because of the stochastic nature of the renewable, particularly wind power, accurate forecast is very difficult. Hence, the effort is made to minimize the effects of forecast errors and obtain a reliable data about the renewable power to be applied to the UC.

In order to model the uncertainty of the renewable power forecast, the dependable generation should be calculated and considered in the scheduling decisions. The forecast error of wind and solar power is likely normally distributed especially for a long-term operation [17]. The maximum error of the forecast is referred to as the value at risk, named $\text{Power}_{\text{risk,max}}$. The concept is the same as the value at risk in financial risk management [18]. The value at risk can be estimated with a level of confidence (LC) which is specified by the generation planners [15]. For example, a 90% LC conveys that the probability of forecasting error ($\text{Power}_{\text{risk}}$) being greater than the value of $\text{Power}_{\text{risk,max}}$ is less than 10%. To implement the risk constraint introduced by (9), it requires to compute the value of $\text{Power}_{\text{risk,max}}$ from the given LC and the PDF of the forecast error. The most important risk occurs when the renewable power is overestimated (i.e., when the real-time actual generation is less than the forecasted level), thus, the upper side of the distribution curve is considered. The value of $\text{Power}_{\text{risk,max}}$ is subtracted from the generation forecast data and the resultant dependable capacity is counted in the UC. $\text{Power}_{\text{risk,max}}$ is estimated as follows:

$$\alpha = 100 - \text{LC}, \tag{15}$$

$$P[e \geq \mu_e + z_\alpha \sigma_e] < \frac{\alpha}{100}. \tag{16}$$

The minimum error value (e) by which (16) can be satisfied will be referred to as the $\text{Power}_{\text{risk,max}}$, given by (Figure 3)

$$\text{Power}_{\text{risk,max}} = \widetilde{e} = \mu_e + z_\alpha \sigma_e, \tag{17}$$

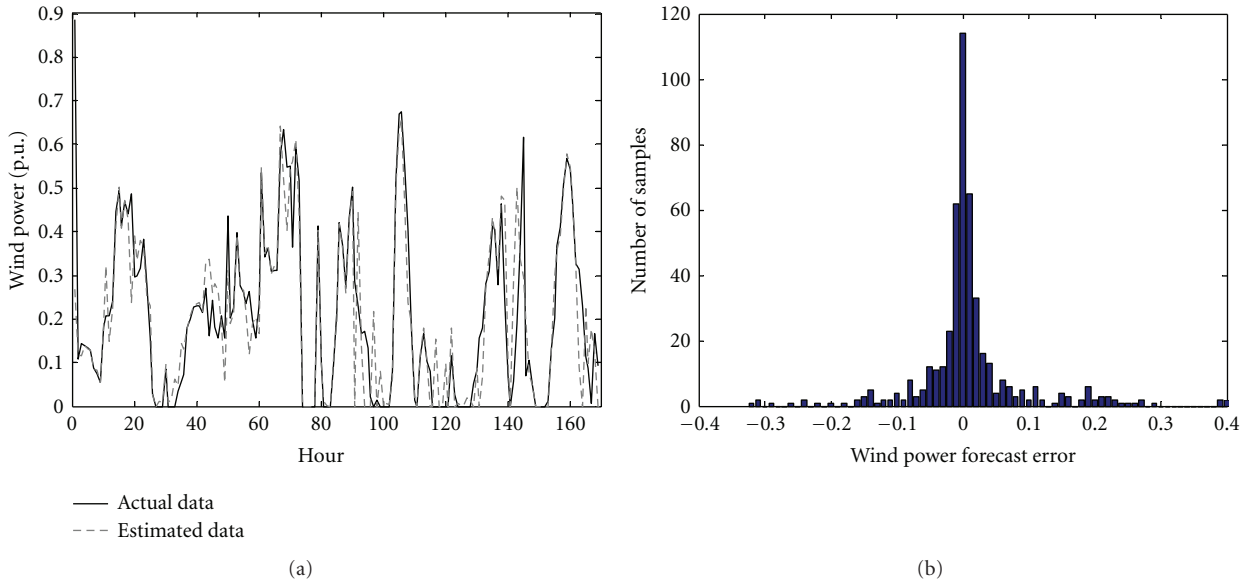

Figure 1: (a) Actual and estimated wind power. (b) Distribution of wind power forecast error from the applied NN model.

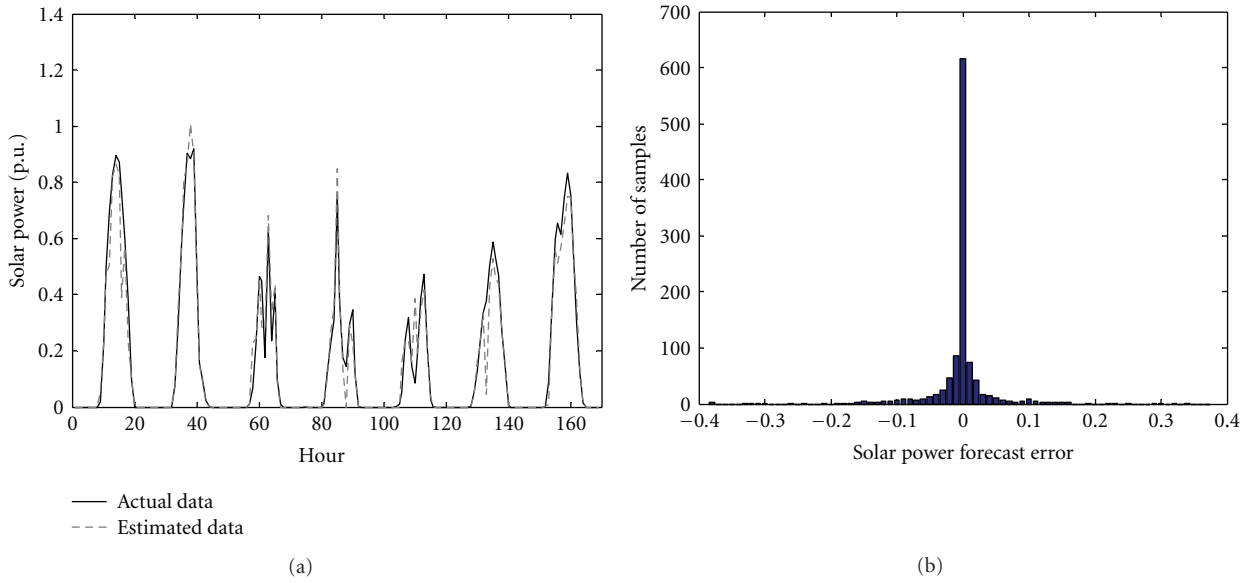

Figure 2: (a) Actual and estimated solar power. (b) Distribution of solar power forecast error from the applied NN model.

where z_α is the variance coefficient to express $\tilde{e}$ in terms of the mean and standard deviation for a normal PDF approximation.

4. Applied Optimization Method

4.1. Differential Evolution Algorithm. Differential evolution algorithm, introduced by Price et al. [19], is a simple population-based, stochastic evolutionary algorithm for global optimization and is capable of handling nondifferentiable, nonlinear and multimodal objective functions [20]. In DEA, the population consists of real-valued vectors with dimension D that equals the number of design parameters. The population size is adjusted by the parameter N_P [19]. The initial population is uniformly distributed in the search space. Each variable x_k in an individual i is initialized within its boundaries $x_{k,\min}$ and $x_{k,\max}$. After the initialization step, the algorithm yields the optimization solution through the following iterative steps.

(1) Mutation. A mutant vector for each target vector $(X_{i,G})$ of the current population is generated by the mutation operator, as follows:

$$V_{i,G+1} = X_{r1,G} + F \cdot (X_{r2,G} - X_{r3,G}), \tag{18}$$

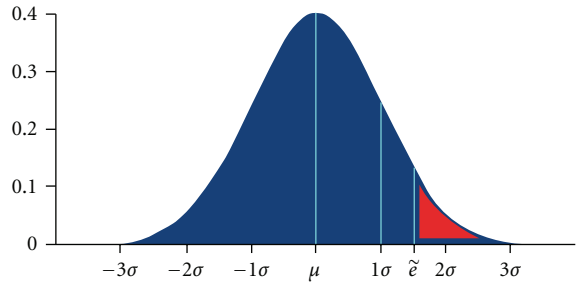

Figure 3: Computation of the confidence interval using the forecast error PDF.

where $X_{ri,G}$ is a randomly chosen vector among the population in the generation G; F is a constant within $(0, 2)$; $V_{i,G+1}$ is the mutant vector. In (18), if $X_{r1,G}$ is replaced by $X_{\text{best},G}$, which is the vector of lowest objective function value from the current population, another form of the presented DE (R-DE) called B-DE will be formed.

(2) Crossover. The crossover operator generates a new vector, called trial vector. The trial vector takes the elements of the target vector $(X_{i,G})$ and mutant vector $(V_{i,G+1})$ with the probability of crossover constant (CR) [21]:

$$U_{i,G+1} = \begin{cases} V_{i,G+1}, & \text{if } \text{rand}_i \le \text{CR or } \text{rand}_j = i \\ X_{i,G}, & \text{otherwise,} \end{cases} \tag{19}$$

where rand_i is a random number in the interval $(0, 1)$ and rand_i is a random index selected among the dimension of decision variable vectors $(1, \ldots, D)$.

(3) Selection (Replacement). Each individual of the new population is compared to the corresponding individual of the previous population, and the best of them is selected as a member of the population in the next generation (elitism). The resultant individuals $X_{i,G+1}$ are admitted to the next iteration:

$$X_{i,G+1} = \begin{cases} U_{i,G+1}, & \text{if } f(U_{i,G+1}) < f(X_{i,G}), \\ X_{i,G}, & \text{otherwise,} \end{cases} \quad i \in [1, N_P]. \tag{20}$$

The iterative steps continue until the convergence criterion is satisfied or a specified number of iterations is completed. The algorithm is further illustrated in Figure 4.

4.2. Implementation. Each individual vector in DE consists of a sequence of integers representing on/off status of generation units in the operating cycles during the planning period. Therefore, each solution is a vector of $N \times C$ variables for a system with N units and planning period divided into C cycles. The program is developed in MATLAB programming environment. The DE has an initial population of 50 solutions and is run for 100 iterations.

The minimum up- and down-time constraints are satisfied with no need to penalty functions, as described in [11]. After satisfying time constraints and before the selection step of DE, the generation levels P_i^t of the on-state units at each time step of the planning period are determined by performing economic dispatch as a nested optimization loop to minimize the total fuel cost [10]. The fitness function will be calculated using the calculated P_i of units.

5. Case Study and Simulation Results

The case study is implemented on conventional 10-unit test system for the UC. The data for load and units of this system are presented in Tables 1 and 2 [10, 14]. A wind and a PV unit are incorporated in the system, yielding totally 12 units. The available data for wind speed and solar irradiation which are transformed to power data is assumed as an aggregated generation from Ardebil city in the north west of Iran from January to December of 2005. The considered wind (unit 11) and PV (unit 12) capacities are 180 MW and 45 MW, respectively. The spinning reserve requirement is assumed to be 10% of the total load. Table 3 depicts the result of generation scheduling of the supreme solution of DE for the described test system. Each cell shows the amount of power generation by each unit in the corresponding hour of the 24 hour schedule.

To show the effectiveness of DE, GA [14] with the same population size and number of iterations is employed as a reference. As a comparison, this method has better convergence over than genetic algorithm (GA) as one of the well-known powerful intelligent methods. Table 4 shows this comparison in both cases of with and without renewable power penetration.

The risk constraint of renewable power has been implemented considering the LC to be 90%. The forecast error distribution of wind and solar power was shown in Figures 1(b) and 2(b), respectively. From these figures, the mean of the forecast error is zero and the error is well accumulated around the mean. By analyzing the forecast error distributions, the risk constraint implies the reduction of $\text{Power}_{\text{risk,max}}$, namely, 0.03 p.u. from the forecasted wind power and 0.016 p.u. from the forecasted solar power for the case of normal distribution. Then, the resultant data are input as the dependable generation of the PV and wind units. Figure 5 depicts how the estimated value at risk has been subtracted from the forecasted generation for 90% and 95% level of confidence. The dependable generation is reduced when a higher level of confidence is considered but ensures the system operators that the planned generation can be reached in real-time more confidently.

6. Conclusion

Ever increasing penetration of intermittent renewable generations into the existing power systems reveals new reliability and security issues to the power system planners and operators. In this paper, the impact of the uncertain nature of solar and wind power on planning and dispatch of

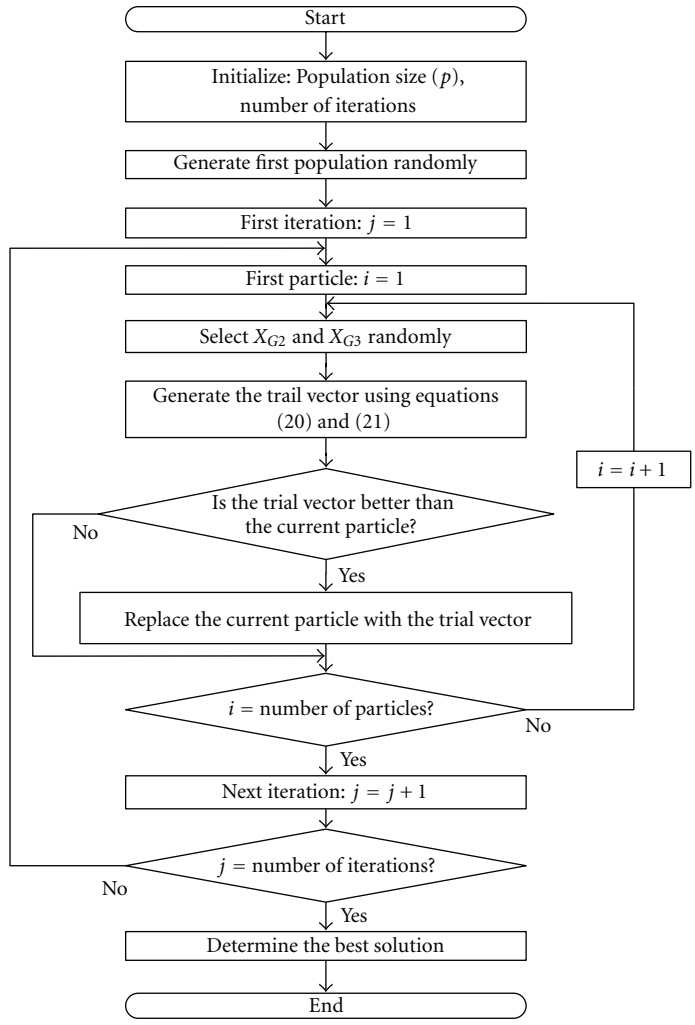

Figure 4: Flowchart of DE Algorithm.

Table 1: Load demand for 24 hours.

Hour [h]	1	2	3	4	5	6	7	8	9	10	11	12
Demand [MW]	700	750	850	950	1000	1100	1150	1200	1300	1400	1450	1500
Hour [h]	13	14	15	16	17	18	19	20	21	22	23	24
Demand [MW]	1400	1300	1200	1050	1000	1100	1200	1400	1300	1100	900	800

Table 2: Operator data for ten thermal units in the system.

	Unit 1	Unit 2	Unit 3	Unit 4	Unit 5	Unit 6	Unit 7	Unit 8	Unit 9	Unit 10
$P_{i\max}$	455	455	130	130	162	80	85	55	55	55
$P_{i\min}$	150	150	20	20	25	20	25	10	10	10
A_i	1000	970	700	680	450	370	480	660	665	670
B_i	16.19	17.26	16.60	16.50	19.70	22.26	27.74	25.92	27.27	27.79
C_i	0.00048	0.00031	0.002	0.00211	0.00398	0.00712	0.00079	0.00413	0.00222	0.00173
MU_i	8	8	5	5	6	3	3	1	1	1
MD_i	8	8	5	5	6	3	3	1	1	1
HS_i	4500	5000	550	560	900	170	260	30	30	30
CS_i	9000	10000	1100	1120	1800	340	520	60	60	60
CSH_i	5	5	4	4	4	2	2	0	0	0
Init. state	8	8	−5	−5	−6	−3	−3	−1	−1	−1

Table 3: Unit schedule in 24 hours and operation costs.

Hour	Power generation of units (MW)												Generation cost ($)	Start up cost ($)
	1	2	3	4	5	6	7	8	9	10	11	12		
1	403.83	150	0	0	0	0	0	0	0	0	146.164	0	11182.36	0
2	455	164.484	0	0	0	0	0	0	0	0	130.515	0	12283.21	0
3	455	246.849	0	0	0	0	0	0	0	0	148.150	0	13715.33	0
4	455	335.784	0	0	0	0	0	0	0	0	159.215	0	15266.41	0
5	455	392.241	0	0	0	0	0	0	0	0	152.758	0	16253.61	0
6	455	377.552	130	0	0	0	0	0	0	0	137.447	0	18888.36	1100
7	455	421.606	130	0	0	0	0	0	0	0	143.393	0	19659.66	0
8	455	451.134	130	0	0	20	0	0	0	0	140.825	3.04	20995.35	340
9	455	455	130	0	0	80	0	12.437	0	0	150.843	16.72	23424.47	60
10	455	455	130	130	0	65.287	0	0	0	0	138.672	26.04	24959.4	1120
11	455	455	130	130	0	74.301	25	0	0	10	137.778	32.92	27291.08	580
12	455	455	130	130	0	80	54.857	0	0	0	157.063	38.08	27306.24	0
13	455	455	130	130	0	0	26.978	0	0	10	153.581	39.44	25282.8	60
14	455	408.662	130	130	0	0	0	0	0	0	139.257	37.08	22293.57	0
15	455	453.295	0	130	0	0	0	10	0	0	120.384	31.32	21103.68	60
16	455	313.709	0	130	0	0	0	0	0	0	128.330	22.96	17741.61	0
17	455	261.078	0	130	0	0	0	0	0	0	141.441	12.48	16823.82	0
18	455	358.129	0	130	0	0	0	0	0	0	156.230	0.64	18517.56	0
19	455	434.034	0	130	25	0	0	0	0	0	155.965	0	20791.31	1800
20	455	455	130	130	74.0957	0	0	0	0	0	155.904	0	25037.3	1100
21	455	455	130	0	106.744	0	0	0	0	0	153.255	0	22843.32	0
22	455	330.949	130	0	25	0	0	0	0	0	159.050	0	19018.76	0
23	455	0	130	0	159.261	0	0	0	0	0	155.738	0	15046.02	0
24	455	0	130	0	58.1027	0	0	0	0	0	156.897	0	12965.68	0
						Total							468690	6620

Table 4: Comparison of best result of DE with GA in thermal and renewable integrated systems.

Method	Total operation cost ($)	
	With renewable integration	Without renewable integration
GA	509320	565825
DE	475310	564735

the thermal power system is examined. A class of MLP is used to estimate the renewable generation level. Although deterministic approaches use a point forecast of the power output, the risk associated with wind and solar power is derived from the mismatch between the historical predicted data and the measured data. On this basis, the hourly dependable generation of solar and wind power is input to the UC problem to satisfy the reliability needs of the power system operator. The resultant risk constraint is considered to reach a compromise between system security and total operation cost. By this approach, the need to evaluate different stochastic scenarios for the wind and solar power in the optimization process is also eliminated and the computational burden is reduced. The risk-constrained UC problem is solved using differential evolution algorithm and the optimal day ahead scheduling of the dispatchable units is obtained. Simulation results indicate the effectiveness of the method for the integration of PV and wind power in the UC problem.

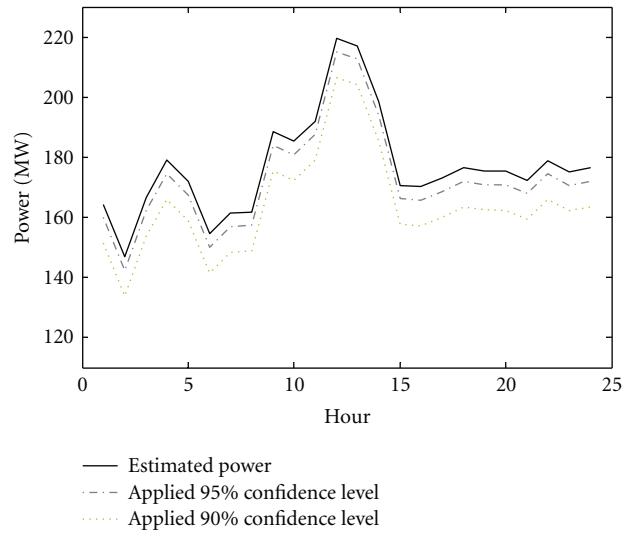

Figure 5: Estimated renewable power and applied power into UC with 90% and 95% confidence level.

Nomenclature

$P^t_{i\min}$: Minimum output power of ith unit at hour t
$P^t_{i\max}$: Maximum output power of ith unit at hour t
$P_{i\min}$: Minimum rated generation level of unit i
$P_{i\max}$: Maximum rated generation capacity of unit i
P^t_i: Output power of ith unit at hour t
τ: The UC time step, equals 60 min
RD_i: Ramp-down rate of unit i
RU_i: Ramp-up rate of unit i
$T^t_{i\text{on}}$: The period during which the ith unit is continuously on
$T^t_{i\text{off}}$: The period during which the ith unit is continuously off
MUT_i: Maximum up-time limit of unit i
MDT_i: Minimum down-time limit of unit i
$u_i(t)$: Operation status of unit i at hour t (1 = ON, 0 = OFF)
$P_{C,\text{RES}}(t)$: The confident level of power available from PV and wind units at hour t
D^t: System load demand at hour t
R^t: System reserve at hour t
A_i, B_i, C_i: The fuel cost function coefficients
CSH_i: Cold start hour of unit i
HS_i: Hot start cost of unit i
CS_i: Cold start cost of unit i
SU_i: Start-up cost for unit i
SD_i: Shutdown cost for unit i
$R(\cdot)$: Unit ramp function
$e^{\sim}$: The value at risk of the estimated
μe: Mean value of the data forecast error
σe: Standard deviation of the forecasted data.

References

[1] E. Constantinescu, V. Zavala, M. Rocklin, S. Lee, and M. Anitescu, "Unit commitment with wind power generation: integrating wind forecast uncertainty and stochastic programming," Argonne National Laboratory (ANL), 2009.

[2] R. E. P. Framework, "Renewables global status report: 2009 update," *Renewable Energy World*, 2009.

[3] M. Shahidehpour and F. Schwarts, "Don't let the sun go down on PV [photovoltaic systems]," *Power and Energy Magazine*, vol. 2, pp. 40–48, 2004.

[4] T. O. Ting, M. V. C. Rao, and C. K. Loo, "A novel approach for unit commitment problem via an effective hybrid particle swarm optimization," *IEEE Transactions on Power Systems*, vol. 21, no. 1, pp. 411–418, 2006.

[5] M. Shahidehpour, H. Yamin, and Z. Li, *Market Operations in Electric Power Systems*, Wiley, New York, NY, USA, 2002.

[6] V. P. Pappala, I. Erlich, K. Rohrig, and J. Dobschinski, "A stochastic model for the optimal operation of a wind-thermal power system," *IEEE Transactions on Power Systems*, vol. 24, no. 2, pp. 940–950, 2009.

[7] N. P. Padhy, "Unit commitment—a bibliographical survey," *IEEE Transactions on Power Systems*, vol. 19, no. 2, pp. 1196–1205, 2004.

[8] R. C. Johnson, H. H. Happ, and W. J. Wright, "Large scale hydro-thermal unit commitment-method and results," *IEEE Transactions on Power Apparatus and Systems*, vol. PAS-90, no. 3, pp. 1373–1384, 1971.

[9] H. H. Balci and J. F. Valenzuela, "Scheduling electric power generators using particle swarm optimization combined with the Lagrangian relaxation method,," *International Journal of Applied Mathematics and Computer Science*, vol. 14, pp. 411–422, 2004.

[10] I. G. Damousis, A. G. Bakirtzis, and P. S. Dokopoulos, "A solution to the unit-commitment problem using integer-coded genetic algorithm," *IEEE Transactions on Power Systems*, vol. 19, no. 2, pp. 1165–1172, 2004.

[11] J. Ebrahimi, S. H. Hosseinian, and G. B. Gharehpetian, "Unit commitment problem solution using shuffled frog leaping algorithm," *IEEE Transactions on Power Systems*, vol. 26, pp. 573–581, 2010.

[12] C. L. Chen, "Optimal wind-thermal generating unit commitment," *IEEE Transactions on Energy Conversion*, vol. 23, no. 1, pp. 273–280, 2008.

[13] A. Tuohy, P. Meibom, E. Denny, and M. O'Malley, "Unit commitment for systems with significant wind penetration," *IEEE Transactions on Power Systems*, vol. 24, no. 2, pp. 592–601, 2009.

[14] S. A. Kazarlis, A. G. Bakirtzis, and V. Petridis, "A genetic algorithm solution to the unit commitment problem," *IEEE Transactions on Power Systems*, vol. 11, no. 1, pp. 83–92, 1996.

[15] K. Methaprayoon, C. Yingvivatanapong, W. J. Lee, and J. R. Liao, "An integration of ANN wind power estimation into unit commitment considering the forecasting uncertainty," *IEEE Transactions on Industry Applications*, vol. 43, no. 6, pp. 1441–1448, 2007.

[16] A. Mellit and S. A. Kalogirou, "Artificial intelligence techniques for photovoltaic applications: a review," *Progress in Energy and Combustion Science*, vol. 34, no. 5, pp. 574–632, 2008.

[17] L. Soder, "Reserve margin planning in a wind-hydro-thermal power system," *IEEE Transactions on Power Systems*, vol. 8, no. 2, pp. 564–570, 1993.

[18] P. Jorion, *Value at Risk: The New Benchmark for Managing Financial Risk*, McGraw–Hill, New York, NY, USA, 2007.

[19] K. V. Price, R. M. Storn, and J. A. Lampinen, *Differential Evolution: A Practical Approach to Global Optimization*, Springer, New York, NY, USA, 2005.

[20] M. Varadarajan and K. S. Swarup, "Differential evolutionary algorithm for optimal reactive power dispatch," *International Journal of Electrical Power and Energy Systems*, vol. 30, no. 8, pp. 435–441, 2008.

[21] R. Storn and K. Price, "Differential evolution–a simple and efficient heuristic for global optimization over continuous spaces," *Journal of Global Optimization*, vol. 11, no. 4, pp. 341–359, 1997.